

2009

Anthropogenic Osmium in Rain and Snow Reveals Global-Scale Atmospheric Contamination

Cynthia Chen

Peter N. Sedwick

Old Dominion University, Psedwick@odu.edu

Mukul Sharma

Follow this and additional works at: https://digitalcommons.odu.edu/oeas_fac_pubs

 Part of the [Atmospheric Sciences Commons](#), [Biogeochemistry Commons](#), [Environmental Chemistry Commons](#), [Environmental Health and Protection Commons](#), and the [Oceanography Commons](#)

Repository Citation

Chen, Cynthia; Sedwick, Peter N.; and Sharma, Mukul, "Anthropogenic Osmium in Rain and Snow Reveals Global-Scale Atmospheric Contamination" (2009). *OEAS Faculty Publications*. 87.
https://digitalcommons.odu.edu/oeas_fac_pubs/87

Original Publication Citation

Chen, C., Sedwick, P.N., & Sharma, M. (2009). Anthropogenic osmium in rain and snow reveals global-scale atmospheric contamination. *Proceedings of the National Academy of Sciences of the United States of America*, 106(19), 7724-7728. doi: 10.1073/pnas.0811803106

Anthropogenic osmium in rain and snow reveals global-scale atmospheric contamination

Cynthia Chen^a, Peter N. Sedwick^b, and Mukul Sharma^{a,1}

^aRadiogenic Isotope Geochemistry Laboratory, Department of Earth Sciences, Dartmouth College, 6105 Sherman Fairchild Hall, Hanover, NH 03755; and ^bDepartment of Ocean, Earth and Atmospheric Sciences, Old Dominion University, 4600 Elkhorn Avenue, Norfolk, VA 23529

Edited by Karl K. Turekian, Yale University, New Haven, CT, and approved March 27, 2009 (received for review November 19, 2008)

Osmium is one of the rarer elements in seawater, with typical concentration of $\approx 10 \times 10^{-15} \text{ g g}^{-1}$ ($5.3 \times 10^{-14} \text{ mol kg}^{-1}$). The osmium isotope composition ($^{187}\text{Os}/^{188}\text{Os}$ ratio) of deep oceans is 1.05, reflecting a balance between inputs from continental crust (≈ 1.3) and mantle/cosmic dust (≈ 0.13). Here, we show that the $^{187}\text{Os}/^{188}\text{Os}$ ratios measured in rain and snow collected around the world range from 0.16 to 0.48, much lower than expected (>1), but similar to the isotope composition of ores (≈ 0.2) that are processed to extract platinum and other metals to be used primarily in automobile catalytic converters. Present-day surface seawater has a lower $^{187}\text{Os}/^{188}\text{Os}$ ratio (≈ 0.95) than deep waters, suggesting that human activities have altered the isotope composition of the world's oceans and impacted the global geochemical cycle of osmium. The contamination of the surface ocean is particularly remarkable given that osmium has few industrial uses. The pollution may increase with growing demand for platinum-based catalysts.

pollution | seawater | isotopes | platinum group metals | precipitation

The introduction of automobile catalytic converters has substantially reduced emissions of NO_x , CO , and short-chained hydrocarbons over the last 30 years. However, an unintended consequence of using catalytic converters is that the platinum group elements (PGEs: Os, Ir, Pt, Pd, Ru, Rh) are now polluting the environment (1). Although most of fine particulate matter from automobile exhaust containing PGEs settles close to highways and in urban areas (e.g., refs. 2 and 3), increasing PGE concentrations have been noted in ice cores (1, 4) and snow (5–7) in remote regions. In general, all PGEs are immobile (8) except Os, which can form volatile OsO_4 during high-temperature industrial processes such as smelting of concentrated ores (9). Anthropogenic Os has been observed in estuaries (10, 11), coastal sediments (12, 13), and lakes (3). Aerially transmitted anthropogenic Os has been observed near chromium smelters (14) and in urban areas (11, 15), where likely sources are hospital incinerators (10, 16) and automobile catalytic converters (17). Smelters and incinerators represent a local contamination source, whereas automobile catalytic converters could potentially provide a much larger source of globally dispersed Os. The key issues are the extent to which the anthropogenic Os is dispersed and whether this is impacting the natural geochemical cycle of Os. If the natural budget of Os has been disturbed by human activity, then Os isotopes could be a valuable tracer for the hydrological cycle, similar to Pb from leaded gasoline usage before 1978 or tritium from atmospheric atomic bomb testing in the early 1960s. Here, we examine these questions by measuring Os in surface waters.

Deep seawater has an Os $^{187}\text{Os}/^{188}\text{Os}$ of 1.05 ± 0.01 , reflecting a balance between riverine and cosmic and/or hydrothermal sources (18–21). Because radiogenic ^{187}Os is produced from the β -decay of ^{187}Re (half-life = 42 billion years), the $^{187}\text{Os}/^{188}\text{Os}$ of potential atmospheric sources of Os vary considerably, depending on their Re/Os and the time elapsed after their formation (Fig. 1). Os isotope compositions closer to 0.1 are considered “unradiogenic,” whereas those closer to 1 are considered “ra-

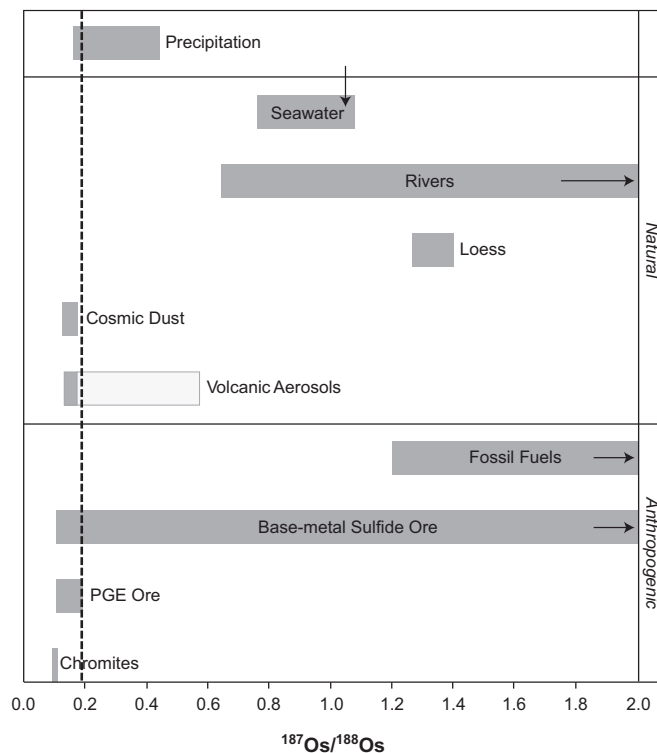


Fig. 1. Comparison of the Os isotope ratios of potential atmospheric sources with values measured in precipitation. Dashed line represents the unradiogenic endmember estimated from the y-intercept of the mixing line (Fig. 2). The arrow in seawater range marks the average $^{187}\text{Os}/^{188}\text{Os}$ ratio of deep-ocean water. The lighter box on the volcanic aerosols represents values estimated from island arc rocks. Rivers, fossil fuels, and base-metal sulfide ores have $^{187}\text{Os}/^{188}\text{Os}$ values that exceed 2. Data references are: precipitation (this study and refs. 25 and 53), seawater (this study and refs. 18–20 and 48), rivers (25, 54), loess (22, 23), cosmic dust (19, 55), volcanic aerosols (24–26), fossil fuels (27, 28), base-metal sulfide ores (30–32), PGE ores (29), and chromites (33).

diogenic.” Natural sources of Os to the atmosphere include continental mineral aerosols ($^{187}\text{Os}/^{188}\text{Os} = 1.26$) (22, 23), cosmic dust ($^{187}\text{Os}/^{188}\text{Os} = 0.13$) (19), and volcanic aerosols. There are limited data on the Os isotope composition of volcanic aerosols; direct measurements from Mauna Loa (Hawaii) give a value of 0.14 (24). However, aerosols from volumetrically dominant eruptions at the convergent margins are likely to be more radiogenic: Analyses of a large number of volcanic rocks from

Author contributions: C.C. and M.S. designed research; C.C. and P.N.S. performed research; C.C. and M.S. analyzed data; and C.C. and M.S. wrote the paper.

The authors declare no conflict of interest.

This article is a PNAS Direct Submission.

¹To whom correspondence should be addressed. E-mail: mukul.sharma@dartmouth.edu.

This article contains supporting information online at www.pnas.org/cgi/content/full/0811803106/DCSupplemental.

Table 1. Osmium concentrations and isotopic compositions in rain, snow, and seawater

Parameter	Coordinates	[Os], fg g ⁻¹	[Os] _c [†] , fg g ⁻¹	¹⁸⁷ Os/ ¹⁸⁸ Os [‡]	[¹⁸⁷ Os/ ¹⁸⁸ Os] _c [†]
Precipitation					
North America					
Alaska	65°9'N, 147°29'W	0.35 ± 0.01	0.28 ± 0.02	0.386 ± 0.006	0.42 ± 0.01
California (Soda Springs), snow	39°23'N, 120°27'W	2.94 ± 0.02	2.9 ± 0.1	0.204 ± 0.003	0.202 ± 0.003
Montana	45°35'N, 107°26'W	0.33 ± 0.01	0.25 ± 0.01	0.402 ± 0.006	0.441 ± 0.008
Ohio, rain	40°47'N, 80°55'W	0.600 ± 0.004	0.53 ± 0.03	0.337 ± 0.006	0.346 ± 0.005
Florida, rain	27°22'N, 82°17'W	0.931 ± 0.005	0.86 ± 0.04	0.278 ± 0.006	0.279 ± 0.006
New Hampshire (Hanover), snow	43°42'N, 72°17'W	17.0 ± 0.1	16.9 ± 0.9	0.164 ± 0.003	0.163 ± 0.002
New Hampshire (Hanover), rain	43°43'N, 72°15'W	0.993 ± 0.006	0.92 ± 0.05	0.240 ± 0.006	0.238 ± 0.004
Europe					
Almere, The Netherlands, rain	52°23'N, 5°18'E	5.31 ± 0.03	5.2 ± 0.3	0.275 ± 0.004	0.275 ± 0.004
Asia					
Mangalore, India, rain	12°54'N, 74°50'E	22.9 ± 0.3	23 ± 1	0.160 ± 0.002	0.160 ± 0.002
Antarctica					
Ross Sea (CORSAKS2 IS-1), snow	67°08'S, 174°42'W	1.76 ± 0.01	1.69 ± 0.09	0.198 ± 0.003	0.195 ± 0.003
Ross Sea (CORSAKS2 IS-3), snow	70°19'S, 177°07'W	0.83 ± 0.01	0.76 ± 0.04	0.46 ± 0.01	0.474 ± 0.007
Replicate		0.813 ± 0.006	0.74 ± 0.04	0.458 ± 0.007	0.477 ± 0.007
East Antarctic (SIPEX 10), brine	64°56'S, 119°09'E	11.46 ± 0.06	11.4 ± 0.6	1.02 ± 0.02	1.03 ± 0.01
East Antarctic (SIPEX 10), snow	64°56'S, 119°09'E	3.42 ± 0.02	3.4 ± 0.2	0.97 ± 0.02	0.98 ± 0.01
East Antarctic (SIPEX 11), snow	65°00'S, 117°30'E	0.81 ± 0.01	0.74 ± 0.04	0.362 ± 0.006	0.371 ± 0.005
Seawater					
Surface					
Atlantic Ocean 2007 (25 m)	31°31'N, 63°18'W	9.82 ± 0.08	9.7 ± 0.5	0.76 ± 0.01	0.76 ± 0.01
Atlantic Ocean 2008 (7 m)	31°40'N, 64°10'W	6.22 ± 0.02	6.1 ± 0.3	1.02 ± 0.01	1.03 ± 0.01
Southern Ocean 2006 (6 m)	65°13'S, 174°44'W	9.97 ± 0.08	9.9 ± 0.5	0.956 ± 0.01	0.96 ± 0.01
Indian Ocean 1997 (22 m)*	34°11'S, 55°37'E	–	11.14 ± 0.45	–	1.02 ± 0.04
Pacific Ocean 1997 (25 m)	9°46'N, 104°11'W	8.25 ± 0.10	8.2 ± 0.4	1.01 ± 0.01	1.02 ± 0.01
Deep					
Atlantic Ocean 2007 (2000 m) 20 mL	31°40'N, 64°10'W	8.98 ± 0.07	8.9 ± 0.4	1.03 ± 0.01	1.05 ± 0.01
Replicate		8.90 ± 0.07	8.8 ± 0.4	1.05 ± 0.01	1.06 ± 0.02
Atlantic Ocean 2007 (2000 m) 40 mL	31°40'N, 64°10'W	8.81 ± 0.05	8.8 ± 0.4	1.04 ± 0.01	1.05 ± 0.02
Replicate		8.96 ± 0.03	8.9 ± 0.4	1.04 ± 0.01	1.05 ± 0.02
Atlantic Ocean 2007 (2000 m) 60 mL	31°40'N, 64°10'W	8.67 ± 0.05	8.6 ± 0.4	1.04 ± 0.01	1.04 ± 0.02
Replicate		8.91 ± 0.05	8.7 ± 0.4	1.04 ± 0.01	1.05 ± 0.01
Average deep seawater		8.88 ± 0.12	8.80 ± 0.16	1.041 ± 0.006	1.051 ± 0.006

*Data from ref. 18.

[†]Corrected for a 3.6 ± 0.08 fg blank with ¹⁸⁷Os/¹⁸⁸Os = 0.27 ± 0.032. The given uncertainty reflects uncertainty in the blank determination and counting statistics (Fig. S2).

[‡]Reported uncertainties are the higher of either the external reproducibility of 1.38% or 2 times the standard error from counting statistics.

island arcs suggest that the average ¹⁸⁷Os/¹⁸⁸Os ratio of the aerosols could be ≈0.53 (25), although measurements of Kudryavy volcano show gas condensates to be less radiogenic (0.122–0.152) than the volcanic rocks (0.205–0.588) (26).

Potential anthropogenic sources of Os to the atmosphere include: (i) combustion of fossil fuels, (ii) smelting of PGE sulfide ores, (iii) smelting of base-metal (Cu, Ni, Zn, and Pb) sulfide ores, (iv) smelting of chromium ore, and (v) exhaust from automobile catalytic converters (17). Published ¹⁸⁷Os/¹⁸⁸Os ratios for fossil fuels are highly radiogenic, ranging from 1.2 to 13.7 (27, 28). In contrast, the ¹⁸⁷Os/¹⁸⁸Os of the PGE sulfide ores from the Bushveld Complex, South Africa, are between 0.15 and 0.20 (29). The ¹⁸⁷Os/¹⁸⁸Os of base-metal sulfide deposits are variable; in some cases they are similar to the PGE ores [e.g., Noril'sk, Russia (30), and Yilgarn craton, Australia (31)], and in other cases they are highly radiogenic because of involvement of continental crust in their formation [e.g., Sudbury, Canada (32)]. Chromites of all ages have uniformly low ¹⁸⁷Os/¹⁸⁸Os values, ranging from 0.12 to 0.14 (33). The majority of PGEs are produced in South Africa (Bushveld Complex; ≈70%) and Russia (Noril'sk; ≈25%) (34), therefore the ¹⁸⁷Os/¹⁸⁸Os of automobile exhaust is expected to be 0.15–0.20; direct measurements from catalytic converters give 0.1–0.2 (17).

Results

We measured Os in precipitation samples from North America, Europe, Asia, and Antarctica, and in surface and deep seawater from the North Atlantic, Pacific, and Southern Oceans (Table 1). Os concentrations in precipitation range from 0.25 to 23 fg g⁻¹, averaging 5.7 fg g⁻¹ (1 fg = 10⁻¹⁵ g). The ¹⁸⁷Os/¹⁸⁸Os ratios of these samples are relatively low (0.16–0.48), and fall along a 2-component mixing line (Fig. 2). Several Antarctic snow samples deviate from the mixing line, but this shift to more radiogenic values is likely because of contamination of the snow by brine within the sea ice, because samples with higher salinities have Os concentrations and ¹⁸⁷Os/¹⁸⁸Os ratios closer to those of brine samples. The mixing line in Fig. 2 requires that one source of Os in precipitation to be relatively concentrated with an isotope composition of ¹⁸⁷Os/¹⁸⁸Os ≈0.19, whereas the other Os source would be relatively dilute with ¹⁸⁷Os/¹⁸⁸Os ≥0.48. If the radiogenic endmember were continental mineral dust [¹⁸⁷Os/¹⁸⁸Os = 1.26; (22, 23)], the isotope mass balance indicates that >95% of Os in rain is derived from the unradiogenic source. The ¹⁸⁷Os/¹⁸⁸Os ratios of the surface seawater samples range from 0.76 to 1.03, lower than those measured in deep (≥2,000 m) ocean water, 1.05 ± 0.01 (Table 1 and refs. 18–20). The estimated average ¹⁸⁷Os/¹⁸⁸Os of surface seawater is 0.95. If the

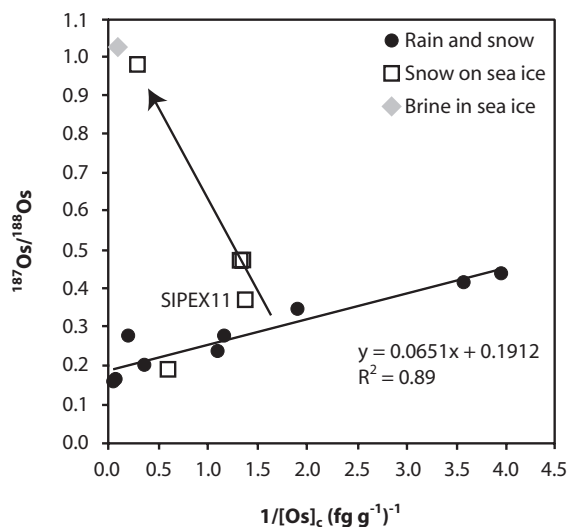


Fig. 2. Plot of $^{187}\text{Os}/^{188}\text{Os}$ versus reciprocal of $[\text{Os}]$ defines a 2-component mixing line for the precipitation data. The unradiogenic endmember has an isotope composition of ≈ 0.19 . Snow collected from sea ice falls on another mixing line between brine and the precipitation mixing line, suggesting that the snow samples are contaminated with brine.

radiogenic endmember in Fig. 2 were surface seawater, the isotope mass balance indicates that $>90\%$ of Os in rain is derived from the unradiogenic source.

Discussion

The low $^{187}\text{Os}/^{188}\text{Os}$ of precipitation implies that sources of highly radiogenic Os cannot contribute the bulk of the Os in precipitation (Fig. 1). Natural sources of unradiogenic Os include meteorites/cosmic dust and volcanism, whereas anthropogenic sources involve processing of sulfide, chromium, and PGE ores and exhaust from automobiles. In the following sections, we examine each of these sources and infer that Os produced during refining of PGE ores likely dominate the isotope signal in precipitation. We then discuss the impact of anthropogenic Os on surface waters.

Natural Sources of Osmium to Precipitation. Cosmic dust and meteorites are unradiogenic (Fig. 1). By using an estimated accretion rate of $0.2\text{--}1.7\text{ g y}^{-1}$ (21), an annual precipitation rate of $5 \times 10^{20}\text{ g y}^{-1}$ (35), and assuming complete dissolution of the cosmic dust, the expected Os concentration of precipitation is $4\text{--}34 \times 10^{-7}\text{ fg g}^{-1}$. The maximum concentration ($34 \times 10^{-7}\text{ fg g}^{-1}$), is much lower than our lowest measured concentration (0.25 fg g^{-1}) for Montana rain. The impact of extraterrestrial Os on the composition of Antarctic snow could be greater if extraterrestrial particles are focused to polar regions (36). The estimated flux of Ir to Antarctica is $4\text{ fg cm}^{-2}\text{ y}^{-1}$ (36). Assuming the Os/Ir ratio of cosmic dust is ≈ 1 and using a net snow accumulation rate of $\approx 30\text{ cm y}^{-1}$ for snow on sea ice, the Os concentration in snow should be $\approx 0.13\text{ fg cm}^{-3}$ ($=\text{ fg g}^{-1}$). However, 0.13 fg g^{-1} is only 18% of the total Os found in our least-concentrated Antarctic snow, SIPEX11 (0.74 fg g^{-1} ; Fig. 2). If Os in SIPEX11 were only a mixture of extraterrestrial dust and seawater, the isotopic mass balance suggests that its $^{187}\text{Os}/^{188}\text{Os}$ would be 0.88. This is much higher than the ratio of 0.37 measured in the SIPEX11 snow. It follows that there must be an additional source of unradiogenic Os to Antarctic snow besides extraterrestrial dust.

That subaerial volcanic activity may provide aerosols with unradiogenic Os is supported by direct measurements of Os isotopes in volcanic emissions from Mauna Loa, Hawaii (24).

The Os isotope composition from Mauna Loa may not be globally representative as the volcanism is associated with hot-spot activity, which contributes only $\approx 5\%$ of total volcanic SO_2 (37). Subduction-zone volcanoes are responsible for $\approx 80\%$ of volcanic SO_2 . Measurements of gas condensate from Kudryavy found them to have lower $^{187}\text{Os}/^{188}\text{Os}$ than the unaltered volcanic rocks (26). Because there is no reason for fractionation of Os isotopes between volcanic aerosols and rocks, the average aerosols likely have Os values closer to ≈ 0.53 (25). If so, subaerial volcanism may not be the primary source of Os in precipitation.

Anthropogenic Contributions of Osmium in Precipitation. Industrial ore processing produces OsO_4 because of high temperatures and oxidizing conditions. In sulfide ore (base-metal and PGE) processing, OsO_4 is generated during the converting phase, where S is removed as SO_2 by the passage of hot air/oxygen through the molten ($900\text{--}1,250\text{ }^\circ\text{C}$) matte that contains mainly metal plus S (9, 38). Scrubbing of the exhaust gases to remove SO_2 appears to nearly quantitatively remove OsO_4 . The majority of OsO_4 is trapped either by the wash sulfuric acid or the slime produced during scrubbing (39). The SO_2 can be used in sulfuric acid production, where the SO_2 is oxidized to SO_3 and then dissolved in H_2SO_4 to form oleum, which is then diluted to form sulfuric acid. Any remaining OsO_4 in the washed SO_2 gas is likely sequestered during sulfuric acid production. The amount of base-metal sulfide ore processed annually is vastly greater than PGE ores, but most base-metal processing facilities appear to scrub for SO_2 (40), whereas PGE ore facilities do not (34). This indicates that processing of PGE ores could release Os observed in precipitation. Indeed, the $^{187}\text{Os}/^{188}\text{Os}$ ratio of the unradiogenic endmember from the mixing trend (Fig. 2) directly matches the isotope composition of PGE ores from Merensky Reef, South Africa and Noril'sk, Russia (Fig. 1). Chromites have high Os contents, and chromite smelters are known to emit Os (14). However, chromites are a less likely source because their Os isotope compositions are much lower than those found in the precipitation samples, and the Os seems to precipitate out close to the source (14). The localized deposition may be due to shorter smokestacks because chromite smelters do not emit SO_2 .

We estimate that Os released from the current production and usage of Pt would result in precipitation with a concentration of $\approx 9\text{ fg g}^{-1}$. This is based on global annual Pt production of 217,000 kg (2005 value) (41) and Pt/Os for PGE ore of ≈ 50 (42), and assuming all Os in PGE ore was volatilized to the atmosphere and ended up in precipitation during production and/or use. It is of the same order of magnitude as the Os concentrations measured in our precipitation samples. Both the exhaust from automobile catalytic converters (17) and the refining of PGEs could provide Os to the atmosphere with the same $^{187}\text{Os}/^{188}\text{Os}$ ratio as that inferred for the unradiogenic precipitation end member. The estimated upper limit of anthropogenic Os flux from automobile exhaust is $\approx 120\text{ pg m}^{-2}\text{ y}^{-1}$ (17), which would result in precipitation with an Os concentration of $\approx 0.1\text{ fg g}^{-1}$. It follows that automobile exhaust provides only a minor source of anthropogenic Os to the atmosphere, with refining of PGEs as the primary source.

That volatility of OsO_4 may be controlling the transport of Os in the atmosphere can be assessed by examining its atmospheric enrichment factor. An atmospheric enrichment factor (AEF) is defined as: $\text{AEF} = \log\{([\text{Os}]_{\text{atm}}/[\text{Al}]_{\text{atm}})/([\text{Os}]_{\text{cont}}/[\text{Al}]_{\text{cont}})\}$, where the subscripts *atm* is atmosphere, and *cont* is upper continental crust. For volatile trace elements, there appears to be a negative relationship between the boiling point of the oxide and its AEF (43), i.e., the lower the boiling point of an element, the higher its AEF. For an OsO_4 boiling point of $135\text{ }^\circ\text{C}$, the

estimated AEF from the trend ranges between 3 and 4. We note that the calculated AEF for Os is 3.6, which is consistent with our inference that atmospheric enrichment of Os is related to its oxidation during refining of PGE-ores.

A disparity between the relative demands for Pt and Os further implicates Pt refining as the primary mechanism by which Os is released to the atmosphere. Examination of PGE consumption figures reveals that the U.S. imported $\approx 106,000$ kg of Pt and 39 kg of Os during 2005 (41). The worldwide production of Pt for the same year was $\approx 217,000$ kg. Because the Pt/Os ratio of the Pt ores is ≈ 50 (42), complete separation of the 2 elements should yield $\approx 4,340$ kg of Os. In comparison, the worldwide consumption of Os is likely to be on the order of 100 kg (41). Thus, there is little incentive to recover the Os lost during the refining of Pt.

Impact of Anthropogenic Osmium on Surface Waters. The quantity of anthropogenic Os that is currently being deposited over the Earth's surface has likely impacted the Os budget of surface waters. Measurements of Os isotopes in paired water and sediment samples from the Connecticut [supporting information (SI) Fig. S1], and the Orinoco (44) Rivers show that the $^{187}\text{Os}/^{188}\text{Os}$ ratio of the water is generally lower than the sediments. Compared with the leachable Os from sediments, the water obtained from the Ganges at Patna also has a lower $^{187}\text{Os}/^{188}\text{Os}$ ratio (45, 46). This isotopic disequilibrium most likely reflects the contribution of anthropogenic Os, which has lowered the $^{187}\text{Os}/^{188}\text{Os}$ ratio of the river waters. In the Orinoco drainage basin, this effect is most obvious in tributaries where chemical weathering is slow and dominated by precipitation. More importantly, some surface seawaters have been found to be lower (Table 1 and refs. 47 and 48) than deep waters (Table 1 and refs. 18–20). Because precipitation is not temporally or spatially evenly distributed over the earth's surface, it is not surprising that not all samples of surface seawater show suppression in $^{187}\text{Os}/^{188}\text{Os}$ values. Additional evidence that the surface oceans have been impacted comes from analyses of modern corals, which fall on a mixing line with an unradiogenic endmember of 0.17 (47); the latter is nearly identical to the unradiogenic endmember of precipitation (Fig. 2).

Assuming that the lower isotope composition observed in surface seawater is caused by anthropogenic Os, we can estimate the flux of anthropogenic Os needed: $J_i = (dR_{SW}/dt)/(R_i - R_{SW}) * N_{SW}$, where $R = ^{187}\text{Os}/^{188}\text{Os}$ ratio, SW and i denote seawater and anthropogenic Os, respectively, and N_{SW} is the total Os inventory of the surface ocean. Given that anthropogenic Os is primarily sourced from PGE production, which is fueled by demand for catalytic converters, we will consider anthropogenic Os contributions over the last 30 years, the length of time that automobile catalytic converters have been in use. Assuming that the atmospheric input of anthropogenic Os has decreased the $^{187}\text{Os}/^{188}\text{Os}$ ratio of the surface mixed layer (depth = 200 m) of the ocean from 1.05 to 0.95, this yields an anthropogenic Os flux of $2,391 \text{ kg y}^{-1}$. In comparison, the estimated emission of anthropogenic Os to atmosphere by the refining of PGEs is $2,657 \text{ kg y}^{-1}$. The remarkable similarity between these fluxes, suggests that the mining and use of PGEs is indeed the source of Os to precipitation, and that human activity may have impacted the global Os budget.

Conclusions

It is ironic that although the phasing out of leaded gasoline and use of catalytic converters has removed Pb and other pollutants from the environment, the processing of Pt used in catalytic converters is polluting the earth's surface with Os. More intriguing is the potential for Os isotopes to be used as

a tracer of hydrologic and oceanographic processes, although this will require more study to confirm and establish the level of contamination of surface seawater. Finally, we conclude that PGE smelters are the primary source of anthropogenic Os and note that the installation of SO_2 scrubbers could greatly reduce atmospheric Os contamination.

Materials and Methods

Sample Collection. Precipitation samples were collected in Hanover, NH, from February 2007–2008, by using acid-cleaned polyethylene receptacles. All other samples are composite samples integrated over multiple rain events. The rain sample from Almere, The Netherlands, was collected February to May 2008 and integrates moisture from a dominant western (Atlantic) rainwater belt. The rain sample from Mangalore, India, was collected from 26 to 30 September 2007 and integrates moisture coming from the Indian Ocean toward the end of the Indian Monsoon season. The Alaska, Montana, Ohio, and Florida precipitation samples were collected by the National Atmospheric Deposition Program from 21–27 October 2007.

The Sierra snow sample was collected at the Central Sierra Snow Laboratory (elevation, 2,100 m) in Soda Springs, CA, by digging a trench in the snowpack with a plastic shovel and then jamming a precleaned high-density polyethylene (HDPE) bottle into the side of the trench. Antarctic snow samples were collected from sea ice in the Ross Sea and off the coast of Wilkes Land, East Antarctica. Snow samples were collected from first year sea ice in acid washed 2-L HDPE bottles. Sea ice brine was pumped from an ice-core hole through acid-washed masterflex tubing, by using a peristaltic pump. Near-surface seawater samples were collected in nonmetal water samplers deployed on a nonmetal line (49). Seawater samples were filtered through $0.4\text{-}\mu\text{m}$ (North Atlantic) or $0.2\text{-}\mu\text{m}$ (Southern Ocean) Pall Supor Acropak filter capsules inside shipboard clean laboratory, and then acidified to $\text{pH} < 2$ by using ultrapure HCl upon return to Dartmouth clean laboratory. All plastics were cleaned by soaking in 20% HNO_3 for > 2 weeks, followed by 10% HCl (trace metal grade) for 24 h.

Chemical Separation and Mass Spectrometry. Approximately 50 g of water and ^{190}Os tracer were preweighed, combined in a quartz glass ampoule, and frozen in a -20°C freezer. To the frozen mixture, 0.5 mL of Jones reagent ($\text{Cr}^{VI}\text{O}_3 + \text{H}_2\text{SO}_4$) was added. The ampoule was then placed in a high-pressure asher (HPA), sealed by applying a confining pressure of 100 bars, and heated to 300°C for 16 h. This allows conversion of all Os to OsO_4 , thus permitting equilibration of tracer and sample Os (46). The ampoule was then removed from the HPA and OsO_4 distilled and trapped in chilled HBr. The resulting hexabromoosmate was further purified by using microdistillation (50). The sample was then dried and loaded onto a high-purity Pt filament and covered with a $\text{Ba}(\text{OH})_2 + \text{NaOH}$ emitter solution.

The Os isotopes were measured as OsO_3^- species (51, 52) on a Triton thermal ionization mass spectrometer by using a secondary electron multiplier operated in ion-counting mode. The ion beams were obtained by using double-filament geometry with a Pt evaporation filament and a Ta heating filament. This geometry provides a stable ion beam and minimizes organic interference on mass 233 ($^{185}\text{ReO}_3^-$), which is used to correct for the isobaric interference on mass 235 ($^{187}\text{OsO}_3^-$) by $^{187}\text{ReO}_3^-$. Repeated analyses ($n = 26$) of the 200-fg MPI Os-1 standard yield an average $^{187}\text{Os}/^{188}\text{Os}$ ratio of $0.1066 \pm 1.38\%$ (2σ), and an $^{190}\text{Os}/^{188}\text{Os}$ ratio of $1.989 \pm 0.32\%$ (2σ) (Fig. S2). The average $^{187}\text{Os}/^{188}\text{Os}$ ratio is within error of the true value of the standard (0.1069); the external reproducibility of the $^{190}\text{Os}/^{188}\text{Os}$ ratio reflects our ability to obtain precise Os concentrations by isotope dilution. The Os blank for the procedure is 3.6 fg, the chemical separation yield for Os $\approx 90\%$, and the ion yield on the mass spectrometer for a 200-fg sample is typically $\approx 5\%$.

ACKNOWLEDGMENTS. We thank the following individuals who provided us samples: North Atlantic GEOTRACES samples [E. A. Boyle, Massachusetts Institute of Technology (MIT)], East Pacific (G. E. Ravizza, University of Hawaii), Almere rain (C. J. Beets, Frei Univ. Amsterdam), Mangalore rain (K. Balakrishna, MIT, India), California snow (R. Osterhuber, CSSL), and North American precipitation (C. Lehmann, NADP). East Antarctic samples were collected by C.C. on SIPEX cruise conducted by the Australian Antarctic Division. We thank A. Bowie for making this possible, and D. Lannuzuel and P. Van der Merwe for help in collecting samples. We thank G. J. Wasserburg for comments and suggestions on an earlier version of this article. Official reviews from 3 anonymous reviewers and K. K. Turekian are gratefully acknowledged because they have led to substantial improvement of the manuscript. This work was supported in part by grants from the National Science Foundation Chemical Oceanography and Antarctic Organisms and Ecosystems Programs.

1. Rauch S, et al. (2005) Importance of automobile exhaust catalyst emissions for the deposition of platinum, palladium, and rhodium in the Northern Hemisphere. *Environ Sci Technol* 39:8156–8162.
2. Ely JC, et al. (2001) Implications of platinum-group element accumulation along U. S. roads from catalytic-converter attrition. *Environ Sci Technol* 35:3816–3822.
3. Rauch S, Hemond HF, Peucker-Ehrenbrink B (2004) Recent changes in platinum group element concentrations and osmium isotopic composition in sediments from an urban lake. *Environ Sci Technol* 38:396–402.
4. Van de Velde K, et al. (2000) Changes in the occurrence of silver, gold, platinum, palladium and rhodium in Mont Blanc ice and snow since the 18th century. *Atmos Environ* 34:3117–3127.
5. Barbante C, et al. (2001) Greenland snow evidence of large scale atmospheric contamination for platinum, palladium, and rhodium. *Environ Sci Technol* 35:835–839.
6. Moldovan M, Veschambre S, Amouroux D, Benech B, Donard OFX (2007) Platinum, palladium, and rhodium in fresh snow from the Aspe Valley (Pyrenees Mountains, France). *Environ Sci Technol* 41:66–73.
7. Gregurek D, et al. (1999) Platinum-group elements (Rh, Pt, Pd) and Au distribution in snow samples from the Kola Peninsula, NW Russia. *Atmos Environ* 33:3281–3290.
8. Gagnon ZE, Newkirk C, Hicks S (2006) Impact of platinum group metals on the environment: A toxicological, genotoxic and analytical chemistry study. *J Environ Sci Health A* 41:397–414.
9. Smith IC, Carson BL, Ferguson TL (1974) Osmium: An appraisal of environmental exposure. *Environ Health Perspect* 8:201–213.
10. Turekian KK, Sharma M, Gordon GW (2007) The behavior of natural and anthropogenic osmium in the Hudson River–Long Island Sound estuarine system. *Geochim Cosmochim Acta* 71:4135–4140.
11. Williams G, Marcantonio F, Turekian KK (1997) The behavior of natural and anthropogenic osmium in Long Island Sound, an urban estuary in the eastern US. *Earth Planet Sci Lett* 148:341–347.
12. Esser BK, Turekian KK (1993) Anthropogenic osmium in coastal deposits. *Environ Sci Technol* 27:2719–2724.
13. Ravizza GE, Bothner MH (1996) Osmium isotopes and silver as tracers of anthropogenic metals in sediments from Massachusetts and Cape Cod bays. *Geochim Cosmochim Acta* 60:2753–2763.
14. Rodushkin I, Engstrom E, Sorlin D, Ponter C, Baxter DC (2007) Osmium in environmental samples from Northeast Sweden. Part II. Identification of anthropogenic sources. *Sci Total Environ* 386:159–168.
15. Rauch S, Hemond HF, Peucker-Ehrenbrink B, Ek KH, Morrison GM (2005) Platinum group element concentrations and osmium isotopic composition in urban airborne particles from Boston, Massachusetts. *Environ Sci Technol* 39:9464–9470.
16. Williams GA, Turekian KK (2002) Atmospheric supply of osmium to the oceans. *Geochim Cosmochim Acta* 66:3789–3791.
17. Poirier A, Garipey C (2005) Isotopic signature and impact of car catalysts on the anthropogenic osmium budget. *Environ Sci Technol* 39:4431–4434.
18. Levasseur S, Birck JL, Allegre CJ (1998) Direct measurement of femtomoles of osmium and the Os-187/Os-186 ratio in seawater. *Science* 282:272–274.
19. Sharma M, Papanastassiou DA, Wasserburg GJ (1997) The concentration and isotopic composition of osmium in the oceans. *Geochim Cosmochim Acta* 61:3287–3299.
20. Woodhouse OB, Ravizza G, Kenison-Falkner K, Statham PJ, Peucker-Ehrenbrink B (1999) Osmium in seawater: Vertical profiles of concentration and isotopic composition in the eastern Pacific Ocean. *Earth Planet Sci Lett* 173:223–233.
21. Sharma M, Rosenberg EJ, Butterfield DA (2007) Search for the proverbial mantle osmium sources to the oceans: Hydrothermal alteration of mid-ocean ridge basalt. *Geochim Cosmochim Acta* 71:4655–4667.
22. Esser BK, Turekian KK (1993) The osmium isotopic composition of the continental-crust. *Geochim Cosmochim Acta* 57:3093–3104.
23. Peucker-Ehrenbrink B, Jahn BM (2001) Rhenium-osmium isotope systematics and platinum group element concentrations: Loess and the upper continental crust. *Geochim Cosmochim Acta* 65:2667–2676.
24. Krahenbuhl U, Geissbuhler M, Buhler F, Eberhardt P, Finnegan DL (1992) Osmium isotopes in the aerosols of the mantle volcano Mauna-Loa. *Earth Planet Sci Lett* 110:95–98.
25. Levasseur S, Birck JL, Allegre CJ (1999) The osmium riverine flux and the oceanic mass balance of osmium. *Earth Planet Sci Lett* 174:7–23.
26. Yudovskaya MA, et al. (2008) Behavior of highly-siderophile elements during magma degassing: A case study at the Kudryavy volcano. *Chem Geol* 248:318–341.
27. Selby D, Creaser RA, Dewing K, Fowler M (2005) Evaluation of bitumen as a Re-187-Os-187 geochronometer for hydrocarbon maturation and migration: A test case from the Polar MVT deposit, Canada. *Earth Planet Sci Lett* 235:1–15.
28. Selby D, Creaser RA (2005) Direct radiometric dating of hydrocarbon deposits using rhenium–osmium isotopes. *Science* 308:1293–1295.
29. McCandless TE, Ruiz J (1991) Osmium isotopes and crustal sources for platinum-group mineralization in the Bushveld Complex, South Africa. *Geology* 19:1225–1228.
30. Walker RJ, et al. (1994) Re-Os isotopic evidence for an enriched-mantle source for the Norilsk-type, ore-bearing intrusions, Siberia. *Geochim Cosmochim Acta* 58:4179–4197.
31. Lambert DD, Foster JG, Frick LR, Hoatson DM, Purvis AC (1998) Application of the Re-Os isotopic system to the study of Precambrian magmatic sulfide deposits of Western Australia. *Aust J Earth Sci* 45:265–284.
32. Morgan JW, Walker RJ, Horan MF, Beary ES, Naldrett AJ (2002) Pt-190-Os-186 and Re-187-Os-187 systematics of the Sudbury Igneous Complex, Ontario. *Geochim Cosmochim Acta* 66:273–290.
33. Walker RJ, Prichard HM, Ishiwatari A, Pimentel M (2002) The osmium isotopic composition of convecting upper mantle deduced from ophiolite chromites. *Geochim Cosmochim Acta* 66:329–345.
34. Jones RT (1999) Platinum smelting in South Africa. *South African J Sci* 95:525–534.
35. Berner EK, Berner RA (1996) *Global Environment: Water, Air, and Geochemical Cycles* (Prentice Hall, Upper Saddle River, NJ).
36. Gabrielli P, et al. (2006) A climatic control on the accretion of meteoric and superchondritic iridium-platinum to the Antarctic ice cap. *Earth Planet Sci Lett* 250:459–469.
37. Halmer MM, Schmincke HU, Graf HF (2002) The annual volcanic gas input into the atmosphere, in particular into the stratosphere: A global data set for the past 100 years. *J Volcanol Geotherm Res* 115:511–528.
38. Jones RT (2004) JOM world nonferrous smelter survey, Part II: Platinum group metals. *J Miner Metals Mater Soc* 56:59–63.
39. Abisheva ZS, Zagorognyaya AN, Bukurov TN (2001) Recovery of radiogenic osmium-187 from sulfide copper ores in Kazakhstan. *Platinum Metals Rev* 45:132–135.
40. Goonan TG (2004) Flows of selected materials associated with world copper smelting. *Open-File Report 2004–1395* (U.S. Geological Survey, Washington, DC).
41. George MW (2006) Platinum-group metals. *Minerals Yearbook* (U.S. Geological Survey, Washington, DC).
42. Naldrett AJ (2004) *Magmatic Sulfide Deposits: Geology, Geochemistry and Exploration* (Springer, Berlin) pp 481–612.
43. Mackenzie FT, Wollast R (1977) Sedimentary cycling models of global processes. *The Sea: Ideas and Observations on Progress in the Study of the Seas—Marine Modeling*, eds Goldberg ED, McCave IN, O'Brien JJ, and Steele JH (Wiley-Interscience, New York), Vol 6, pp 739–785.
44. Chen C, Sharma M, Bostick BC (2006) Lithologic controls on osmium isotopes in the Rio Orinoco. *Earth Planet Sci Lett* 252:138–151.
45. Pegram WJ, Esser BK, Krishnaswami S, Turekian KK (1994) The isotopic composition of leachable osmium from river sediments. *Earth Planet Sci Lett* 128:591–599.
46. Sharma M, Wasserburg GJ, Hoffmann AW, Chakrapani GJ (1999) Himalayan uplift and osmium isotopes in oceans and rivers. *Geochim Cosmochim Acta* 63:4005–4012.
47. Levasseur S, Birck JL, Allegre CJ (1999) Osmium isotopic composition of corals: Evidence for multiple sources. *Geochim Cosmochim Acta* 63:1335–1343.
48. Martin CE, Peucker-Ehrenbrink B, Brunskill G, Szymczak R (2001) Osmium isotope geochemistry of a tropical estuary. *Geochim Cosmochim Acta* 65:3193–3200.
49. Sedwick PN, et al. (2005) Iron in the Sargasso Sea (Bermuda Atlantic Time-series Study region) during summer: Eolian imprint, spatiotemporal variability, and ecological implications. *Global Biogeochem Cycles* 19:13.
50. Birck JL, Barman MR, Capmas F (1997) Re-Os isotopic measurements at the femtomole level in natural samples. *Geostandards Newslett* 21:19–27.
51. Creaser RA, Papanastassiou DA, Wasserburg GJ (1991) Negative thermal ion mass spectrometry of osmium, rhenium, and iridium. *Geochim Cosmochim Acta* 55:397–401.
52. Volkening J, Walczyk T, Heumann KG (1991) Osmium isotope ratio determinations by negative thermal ionization mass spectrometry. *Int J Mass Spectrom Ion Processes* 105:147–159.
53. Gannoun A, et al. (2006) The influence of weathering process on riverine osmium isotopes in a basaltic terrain. *Earth Planet Sci Lett* 243:732–748.
54. Peucker-Ehrenbrink B, Ravizza G (2000) The marine osmium isotope record. *Terra Nova* 12:205–219.
55. Walker RJ, et al. (2002) Comparative Re-187-Os-187 systematics of chondrites: Implications regarding early solar system processes. *Geochim Cosmochim Acta* 66:4187–4201.